

Coherent population oscillations and an effective spin-exchange interaction in a \mathcal{PT} symmetric polariton mixture

P.A. Kalozoumis,^{1,2,3} G. M. Nikolopoulos,³ and D. Petrosyan^{3,4}

¹*Materials Science Department, School of Natural Sciences, University of Patras, GR-26504 Patras, Greece*

²*Hellenic American University, 436 Amherst st, Nashua, NH 0306 USA*

³*Institute of Electronic Structure and Laser, FORTH, GR-71110 Heraklion, Crete, Greece*

⁴*A. Alikhanyan National Laboratory, 0036 Yerevan, Armenia*

We study a two-species mixture of exciton-polaritons with self- and cross-interaction nonlinearities in a double well structure, in the presence of relaxation and continuous pumping. We identify the conditions that render the system parity-time (\mathcal{PT}) symmetric, and investigate its dynamic and static properties. We show that the system can exhibit long-term coherent oscillations of populations of the two polaritonic components between the two potential wells, and can simulate the dynamics of a pair of spin-1/2 particles (qubits) in the presence of exchange interaction.

I. INTRODUCTION

Exciton-polaritons are elementary excitations of semiconductor microcavities and constitute hybrid quasiparticles of strongly coupled light (cavity photons) and matter (quantum well excitons) excitations [1, 2], retaining the properties of both constituents. The excitons instill effective interactions inducing polariton nonlinearities, whereas the small effective mass of photons enables Bose-Einstein condensation (BEC) of polaritons at high temperatures [3, 4]. First experimental observations of exciton-polariton BECs have been reported more than a decade ago [5, 6]. Since then, the remarkable properties of the exciton-polariton systems, combined with their high condensation temperatures [7], have motivated much of the research activity in this field. BECs of exciton polaritons have been studied in various geometries, e.g., parabolic traps [8, 9], double-well potentials [10–13], triple wells [14], and 1D and 2D polariton lattices [15–19]. In contrast to relatively stable atomic BECs, the polariton BECs are open quantum systems; they are inherently strongly dissipative and require continuous pumping, e.g., by external laser fields [20].

The dynamics of dissipative systems can be rendered pseudo-Hermitian in the parity-time (\mathcal{PT}) symmetric setup [21–23], where the gain and loss are exactly balanced in a complex potential with the reflection symmetric real part (energy) and reflection antisymmetric imaginary part (gain/loss). Systems with \mathcal{PT} -symmetry have recently attracted much interest in various branches of physics, extending from quantum mechanics [24] and field theory [25] to optics [26–28] and acoustics [29, 30]. Since the experimental realization of the spontaneous \mathcal{PT} symmetry breaking [31, 32], there has been an enormous progress in the field and a multitude of interesting phenomena have been observed, such as, e.g., power oscillations [32], double refraction [33], and non-reciprocal diffraction [34]. The presence of nonlinearity renders \mathcal{PT} symmetric systems even more remarkable, permitting, for example, unidirectional [35] and asymmetric [36, 37] wave propagation in discrete and continuous structures [38–41].

Despite the plethora of different settings, the study of \mathcal{PT} symmetry in polariton structures is still in its infancy and most works address this issue in the single species context [42, 43]. A natural next step is to consider polariton mixtures [44–46] in a \mathcal{PT} symmetric setting where the losses of the polaritons – due to the semiconductor exciton recombination and photon escape for the microcavity – are compensated by gain from the external laser pumping of the exciton population. Here we study a two-species polariton mixture with self- and cross-interaction nonlinearities in a double well structure. We identify the necessary condition imposed on the pumping rate of the reservoirs and their losses to render the polariton mixture \mathcal{PT} symmetric. We construct the corresponding model, analyze its static and dynamic properties, and show that nearly perfect Rabi-like oscillations of the two polariton components between the two wells can be observed in this system in the presence of moderate self- and cross-interactions. This system can then formally be mapped onto a system of two qubits, or spin-1/2 particles, coupled via exchange (XY) interaction. We calculate the fidelity of an effective SWAP gate and quantum state transfer that the system can simulate, despite being an essentially classical system of coupled BECs. Our results can thus have interesting implications for simulations of spin models with polariton lattices.

II. THE EXCITON-POLARITON SYSTEM

We consider a mixture of two species of semiconductor cavity exciton polaritons in a double-well potential, as shown schematically in Fig. 1. Each of the species (+) or (–) represents a polariton composed of a circularly right- or left-polarized cavity photon coupled to a semiconductor exciton transition (σ_+ or σ_-) with the corresponding change of the magnetic quantum number $\Delta m = +1$ or -1 . Starting with the mean-field Gross-Pitaevskii equation for the exciton-polariton BEC in a tight-binding double-well potential, we follow the standard procedure [47] to derive the discrete nonlinear Schrödinger equation for the four-component system represented by the wave-

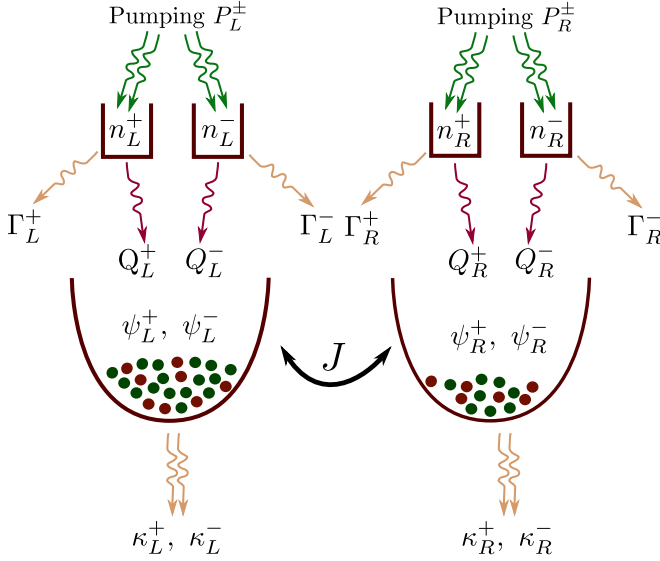


FIG. 1. Schematic representation of a coupled double well potential with a binary mixture of exciton-polaritons $\psi_{L,R}^\pm$. Four exciton reservoirs $n_{L,R}^\pm$ replenish each polariton species (+), (-) in each well (L), (R), respectively. By balancing the polariton loss $\kappa_{L,R}^\pm$ and gain $Q_{L,R}^\pm$ via appropriate reservoir pumping $P_{L,R}^\pm$, we can render the system \mathcal{PT} symmetric.

functions ψ_L^\pm and ψ_R^\pm of the (\pm) species in the left (L) and right (R) wells, respectively,

$$i\hbar\dot{\psi}_L^\pm = \varepsilon_L^\pm\psi_L^\pm + g_s|\psi_L^\pm|^2\psi_L^\pm + g_c|\psi_L^\mp|^2\psi_L^\pm - J\psi_R^\pm + i\frac{\hbar}{2}[Q_L^\pm(n_L^\pm) - \kappa_L^\pm]\psi_L^\pm, \quad (1a)$$

$$i\hbar\dot{\psi}_R^\pm = \varepsilon_R^\pm\psi_R^\pm + g_s|\psi_R^\pm|^2\psi_R^\pm + g_c|\psi_R^\mp|^2\psi_R^\pm - J\psi_L^\pm + i\frac{\hbar}{2}[Q_R^\pm(n_R^\pm) - \kappa_R^\pm]\psi_R^\pm. \quad (1b)$$

Here $\varepsilon_{L,R}^\pm$ are the single-particle energies in each well, g_s and g_c are the self- and cross-interaction strengths of the polaritons, and J is the Josephson tunnel-coupling between the two wells, assumed the same for both species. The complex wavefunctions can be written as $\psi_{L,R}^\pm = \sqrt{N_{L,R}^\pm}e^{i\phi_{L,R}^\pm}$, where $N_{L,R}^\pm \equiv |\psi_{L,R}^\pm|^2$ are the polariton populations and $\phi_{L,R}^\pm$ are the phases. In contrast to an atomic BEC [47], the polariton BEC is a non-conservative system, with the decay $\kappa_{R,L}^\pm$ due the exciton recombination losses and cavity photon losses. The polariton population is continuously replenished via coupling to exciton reservoirs with rates $Q_R^\pm(n_R^\pm)$ [10]. In turn, the exciton populations in each reservoir $n_{R,L}^\pm$ obey the equations

$$\dot{n}_L^\pm = P_L^\pm - \Gamma_L^\pm n_L^\pm - Q_L^\pm(n_L^\pm)N_L^\pm, \quad (2a)$$

$$\dot{n}_R^\pm = P_R^\pm - \Gamma_R^\pm n_R^\pm - Q_R^\pm(n_R^\pm)N_R^\pm, \quad (2b)$$

where $P_{R,L}^\pm$ are the rates of exciton creation, usually induced by a suitable laser pumping [20], $\Gamma_{L,R}^\pm$ are the decay rates of the excitons in the corresponding reservoir,

and $Q_{L,R}^\pm(n_{L,R}^\pm)$ are the rates of stimulated scattering of the reservoir excitons into the condensate of $N_{L,R}^\pm$ polaritons, see Fig. 1. For simplicity, the scattering rate can be approximated by a linear function of the reservoir exciton population, $Q_{L,R}^\pm(n_{L,R}^\pm) \simeq q_{L,R}^\pm n_{L,R}^\pm$ [42].

The model can be further simplified if we assume sufficiently large reservoirs such that the exciton populations remain nearly constant in time, $\dot{n}_L^\pm \simeq 0$, obtaining $n_{L,R}^\pm \simeq \frac{P_{L,R}^\pm}{\Gamma_{L,R}^\pm + q_{L,R}^\pm N_{L,R}^\pm}$. Assuming also that $q_{L,R}^\pm N_{L,R}^\pm \ll \Gamma_{L,R}^\pm$, i.e. the reservoirs are only weakly depleted by the coupling to the polariton condensates, as compared to their strong pumping and decay, we have $n_{L,R}^\pm = P_{L,R}^\pm/\Gamma_{L,R}^\pm$. Upon substitution into Eqs. (1), the polariton gain/loss coefficients become

$$\gamma_{L,R}^\pm = \frac{1}{2}[q_{L,R}^\pm P_{L,R}^\pm/\Gamma_{L,R}^\pm - \kappa_{L,R}^\pm]. \quad (3)$$

Hence, for given polariton decay rates $\kappa_{L,R}^\pm$ – determined by photon losses from the cavity and the spontaneous decay (recombination) of the excitons – and the stimulated scattering $q_{L,R}^\pm$ and decay $\Gamma_{L,R}^\pm$ rates of the reservoir excitons, the polariton gain/loss coefficients $\gamma_{L,R}^\pm$ can be precisely tuned by the laser pumping rates $P_{L,R}^\pm$. In turn, the intensity and spatial distribution of the left- and right-circularly polarized radiation leaking from the cavity is directly proportional to the population $N_{L,R}^\pm$ of the corresponding polariton components and can thus serve for their continuous monitoring [46].

We note that interactions of the polaritons with the reservoir excitons [15, 48] can strongly affect the polariton dynamics, leading to, e.g., instabilities [49], induce the polariton energy shifts and even be used to optically engineer the polariton landscape [46, 50]. But under our assumption of the nearly-constant populations of the exciton reservoirs, their interaction with the polaritons merely leads to a modification of the tight-binding trapping potentials and thereby to constant energy shifts which can be absorbed into $\varepsilon_{L,R}^\pm$.

A one-dimensional system, to be invariant under \mathcal{PT} transformation [21–23], should be confined in a complex potential which has reflection symmetric and reflection antisymmetric real and imaginary parts, respectively. For the coupled-mode equations of the polariton system considered here, these requirements translate to the conditions

$$\varepsilon_L^\pm = \varepsilon_R^\pm, \quad (4a)$$

$$\gamma_L^\pm = -\gamma_R^\pm. \quad (4b)$$

We assume that the system is initially prepared with equal number of particles in each well, $N_L^- + N_L^+ = N_R^- + N_R^+ = N$. We then switch on the tunnel coupling J and increase the reservoir pumping rate near the left well and reduce it near the right, in order to balance gain and loss according to the \mathcal{PT} symmetry condition (4b). The dynamics of the system is governed by the equations

$$i\dot{\psi}_L^\pm = g_s|\psi_L^\pm|^2\psi_L^\pm + g_c|\psi_R^\mp|^2\psi_L^\pm - J\psi_R^\pm + i\gamma\psi_L^\pm, \quad (5a)$$

$$i\dot{\psi}_R^\pm = g_s|\psi_R^\pm|^2\psi_R^\pm + g_c|\psi_L^\mp|^2\psi_R^\pm - J\psi_L^\pm - i\gamma\psi_R^\pm, \quad (5b)$$

where we set $\hbar = 1$ and the zero-point energies $\varepsilon_L^\pm = \varepsilon_R^\pm = 0$, and assumed the balanced gain/loss coefficients equal for both species, $\gamma = \gamma_L^\pm = -\gamma_R^\pm$.

III. \mathcal{PT} SYMMETRY BREAKING AND FIXED POINTS

Let us first review the properties of a linear system with $g_s = g_c = 0$ [31, 32]. The (+) and (-) polaritons decouple from each other and their equations become equivalent. The \mathcal{PT} symmetric and broken phases can be determined from the eigenvalues of the corresponding Hamiltonian matrix, $\Lambda_\pm = \pm\sqrt{J^2 - \gamma^2}$. For $\gamma \leq J$, we have the \mathcal{PT} symmetric phase and the system exhibits pseudo-Hermitian dynamics: each polariton component coherently oscillates between the two wells,

$$\begin{aligned} \begin{bmatrix} \psi_L(t) \\ \psi_R(t) \end{bmatrix} &= U \begin{bmatrix} \psi_L(0) \\ \psi_R(0) \end{bmatrix}, \\ U &= \begin{bmatrix} \cos(\Omega t) + \frac{\gamma}{\Omega} \sin(\Omega t) & i\frac{J}{\Omega} \sin(\Omega t) \\ i\frac{J}{\Omega} \sin(\Omega t) & \cos(\Omega t) - \frac{\gamma}{\Omega} \sin(\Omega t) \end{bmatrix}, \quad (6) \end{aligned}$$

with the effective Rabi frequency $\Omega = (\Lambda_+ - \Lambda_-)/2 = \sqrt{J^2 - \gamma^2}$. When $\gamma > J$, the eigenvalues Λ_\pm become imaginary, the \mathcal{PT} symmetry breaks, and the population of the particles in both wells will diverge exponentially.

In the presence of interactions, $g_s, g_c \neq 0$, the \mathcal{PT} phase diagram cannot be determined from the eigenvalues of non-linear Hamiltonian, but the relevant information can be extracted from the fixed points and their stability properties [39, 51]. Assuming $N_L^+ + N_R^+ = N_L^- + N_R^- = N$, we can recast Eqs. (5) in terms of the polariton population imbalances $z^\pm = (N_L^\pm - N_R^\pm)/N$ and phase differences $\Phi^\pm = \phi_R^\pm - \phi_L^\pm$ as

$$\dot{z}^\pm = -2\sqrt{1 - (z^\pm)^2} \sin \Phi^\pm + 2\frac{\gamma}{J}, \quad (7a)$$

$$\dot{\Phi}^\pm = \frac{g_s}{J}z^\pm + \frac{g_c}{J}z^\mp + 2\frac{z^\pm}{\sqrt{1 - (z^\pm)^2}} \cos \Phi^\pm, \quad (7b)$$

where we use the dimensionless time $\tau = tJ$. The fixed points correspond to the static solutions of these equations, $\dot{z}^\pm = \dot{\Phi}^\pm = 0$. By linearizing the above equations in the vicinity of a fixed point, we find the stability eigenvalues λ_i which determine whether the fixed point is (i) *stable* if all eigenvalues have negative real parts, (ii) *unstable* if one or more eigenvalues have positive real part, and (iii) *elliptic* if all eigenvalues are imaginary. The dependence of the stability eigenvalues on γ thus serves as the phase diagram of the nonlinear polariton system, since it shows when the system diverges and when it follows Hermitian-like dynamics.

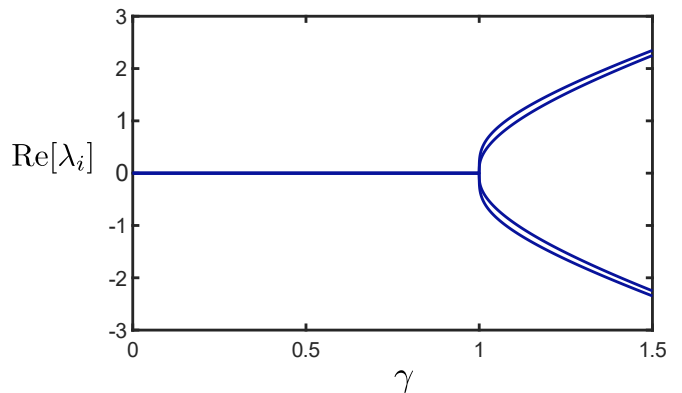


FIG. 2. Real part of the stability eigenvalues λ_i of Eq. (9) around the fixed point (8) as a function of γ , for $g_s N = J$ and $g_c N = 0.9J$. Both axes are in units of J .

A fixed point of the system corresponds to the trivial solution

$$z_1^\pm = 0, \quad \Phi_1^\pm = \pm \arcsin\left(\frac{\gamma}{J}\right), \quad (8)$$

with equal population of the (+) and (-) polaritons in each well. The analytic expression for the four stability eigenvalues is

$$\lambda_i = \pm \frac{\sqrt{-4(J^2 - \gamma^2) - 2(g_s \pm g_c)\sqrt{(J^2 - \gamma^2)}}}{J}. \quad (9)$$

In Fig. 2 we show the real parts of the stability eigenvalues λ_i as a function of γ , for the system prepared in the vicinity of the fixed point (8). We observe only elliptic fixed points, $\text{Re}[\lambda_i] = 0$, where any small deviation leads to oscillations around the fixed point; and unstable fixed points, $\text{Re}[\lambda_i] \neq 0$, in the vicinity of which the system diverges. Equations (9) indicate that as long as $g_s > g_c$ the bifurcation to the unstable eigenvalues occurs when γ reaches a threshold value equal to J . For the values of g_c sufficiently larger than g_s the bifurcation point is shifted to smaller values of γ .

We have examined the possibility of stable fixed points with unequal populations of the two wells, corresponding to, e.g., self-trapping of polariton population on one well [13, 52]. Our analytical and numerical results do not support the existence of such fixed points, as they break the \mathcal{PT} symmetric phase of the system [35, 53].

IV. DYNAMICS OF THE SYSTEM

Before we examine the dynamics of our two-component \mathcal{PT} symmetric system, it is instructive to consider its Hermitian version with $\gamma = 0$. We assume an initial configuration with all (+) particles in the left well and all (-) particles in the right. Figure 3(a) illustrates the corresponding dynamics of population imbalances

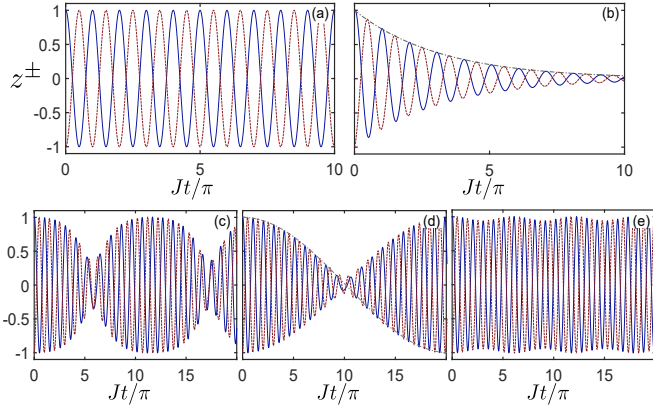


FIG. 3. Dynamics of the population imbalances z^\pm of two polariton species in a double well system, for (a) Hermitian case $\gamma = 0$, (b) non-Hermitian case, with the net gain $\gamma_L = 0.1J$ on the left well and net loss $\gamma_R = -0.2J$ on the right well, and (c,d,e) \mathcal{PT} symmetric cases with balanced gain/loss $\gamma_L = -\gamma_R = \gamma = 0.1J$ on the two wells, and the interaction strengths (c) $g_s N = J$, $g_c N = 0.8J$, (d) $g_s N = g_c N = gN = J$, and (e) $g_s N = J$, $g_c N = 1.2J$. The dash-dotted (gray) line for the amplitude modulation in (b) is $\exp[(\gamma_L + \gamma_R)t]$, and in (d) is $\cos(\frac{\gamma g N}{2J}t)$. Note the different time scales in (a,b) and (c,d,e).

$z^\pm = (N_L^\pm - N_R^\pm)/N$. We observe that the population of each species exhibits Rabi-like oscillations between the two wells with frequency J .

The exciton polariton system is inherently dissipative, which necessitates continuous pumping of polaritons from the exciton reservoirs. In Fig. 3(b) we illustrate the dynamics of the system with the net loss from the right well, $\gamma_R = -0.2J$, being larger than the net gain on the left well, $\gamma_L = 0.1J$. As expected, the polariton populations decay to zero with rate $\gamma_L + \gamma_R$, as do the population imbalances z^\pm normalized to the initial particle number N . In the opposite case of gain being larger than loss, the polariton populations would diverge.

The Hermitian-like dynamics can be achieved with balanced loss and gain, $\gamma_L = -\gamma_R = \gamma$, as per Eqs. (4) corresponding to the \mathcal{PT} symmetric system. Note that the Hermitian system with $\gamma_{L,R} = 0$ can be considered as a special case of the \mathcal{PT} symmetric system with zero imaginary part of the potential. In Fig. 3(c,d,e) we illustrate the dynamics of the interacting system. In the case of $g_s \geq g_c$, the dynamics is characterized by slow modulation of the amplitude of the Rabi-like oscillations between the two wells (see Fig. 3(c)). These modulations are not sinusoidal, exhibiting plateaus of maximal amplitude, followed by rapid collapse and revival of the oscillations. In the case of $g_s = g_c = g$, the modulation amplitude becomes harmonic, with the period well approximated by $T = \frac{4\pi J}{\gamma g N}$ (see Fig. 3(d)). But for moderate interaction strengths $g_s < g_c$, the dynamics is nearly indistinguishable from that of the Hermitian system (see Fig. 3(e)).

V. SIMULATING TWO-QUBIT SWAP GATE

The two-species polariton system in a \mathcal{PT} symmetric double well can be formally mapped onto a system of two qubits, or spin-1/2 particles, coupled via exchange interaction. This is an interesting analogy as it links an essentially classical system described by coupled-mode equations to a quantum system of coupled spins. Here we consider a SWAP gate to simulate state transfer between two qubits.

The complete basis for a system of two qubits (spins) consists of the four states $\{|\downarrow\downarrow\rangle, |\downarrow\uparrow\rangle, |\uparrow\downarrow\rangle, |\uparrow\uparrow\rangle\}$, and an arbitrary two-qubit state $|\Psi\rangle$ can be expanded as

$$|\Psi\rangle = C_{\downarrow\downarrow} |\downarrow\downarrow\rangle + C_{\downarrow\uparrow} |\downarrow\uparrow\rangle + C_{\uparrow\downarrow} |\uparrow\downarrow\rangle + C_{\uparrow\uparrow} |\uparrow\uparrow\rangle. \quad (10)$$

We may associate the (+) component of the polariton in each well $\psi_{L,R}^+$ with the amplitude of the $|\uparrow\rangle$ state of the spin and the (-) component $\psi_{L,R}^-$ with the amplitude of the $|\downarrow\rangle$ state of the spin. Then, the superposition amplitudes in Eq. (10) are given by $C_{\downarrow\downarrow} = c_L^- c_R^-$, $C_{\downarrow\uparrow} = c_L^- c_R^+$, $C_{\uparrow\downarrow} = c_L^+ c_R^-$, $C_{\uparrow\uparrow} = c_L^+ c_R^+$, where $c_L^\pm \equiv \frac{\psi_L^\pm}{\sqrt{|\psi_L^+|^2 + |\psi_L^-|^2}}$ and similarly for $c_R^\pm \equiv \frac{\psi_R^\pm}{\sqrt{|\psi_R^+|^2 + |\psi_R^-|^2}}$.

Our aim is to realize the SWAP gate between the two spins representing qubits. Consider the four input states $|\downarrow\downarrow\rangle, |\downarrow\uparrow\rangle, |\uparrow\downarrow\rangle, |\uparrow\uparrow\rangle$, which can cast as vectors

$$u_{\downarrow\downarrow} = \begin{bmatrix} 1 \\ 0 \\ 0 \\ 0 \end{bmatrix}, u_{\downarrow\uparrow} = \begin{bmatrix} 0 \\ 1 \\ 0 \\ 0 \end{bmatrix}, u_{\uparrow\downarrow} = \begin{bmatrix} 0 \\ 0 \\ 1 \\ 0 \end{bmatrix}, u_{\uparrow\uparrow} = \begin{bmatrix} 0 \\ 0 \\ 0 \\ 1 \end{bmatrix}. \quad (11)$$

In the simplest, non-interacting and Hermitian case, $g_s = g_c = \gamma = 0$ and $J \neq 0$, the dynamics of the system is analytically solvable and for each input state the time-dependent amplitudes of the output state (10) are given in Table I. We observe periodic oscillations of the excitation between the two spins, or qubits, with frequency J . Choosing for the interaction time t half the period of the oscillations, $tJ = \pi/2$, yields the transformation

$$U_{\text{SWAP}} = - \begin{bmatrix} 1 & 0 & 0 & 0 \\ 0 & 0 & 1 & 0 \\ 0 & 1 & 0 & 0 \\ 0 & 0 & 0 & 1 \end{bmatrix}, \quad (12)$$

which is precisely the SWAP gate (with an overall minus sign). For comparison, we recall the dynamics of the coupled spin system governed by the spin-exchange (XY) Hamiltonian $H = -J\hat{\sigma}_L^+ \hat{\sigma}_R^- + \text{H.c.}$, with $\hat{\sigma}^+ = |\uparrow\rangle\langle\downarrow|$ and $\hat{\sigma}^- = |\downarrow\rangle\langle\uparrow|$, for which the initial states $|\downarrow\downarrow\rangle$ and $|\uparrow\uparrow\rangle$ remain unchanged, while the other two basis states evolve as

$$\begin{aligned} |\downarrow\uparrow\rangle &\rightarrow \cos(Jt) |\downarrow\uparrow\rangle + i \sin(Jt) |\uparrow\downarrow\rangle, \\ |\uparrow\downarrow\rangle &\rightarrow \cos(Jt) |\uparrow\downarrow\rangle + i \sin(Jt) |\downarrow\uparrow\rangle. \end{aligned}$$

	$u_{\downarrow\downarrow}$	$u_{\downarrow\uparrow}$	$u_{\uparrow\downarrow}$	$u_{\uparrow\uparrow}$
$C_{\downarrow\downarrow}$	e^{2iJt}	$i \sin(Jt) \cos(Jt)$	$i \sin(Jt) \cos(Jt)$	0
$C_{\downarrow\uparrow}$	0	$\cos^2(Jt)$	$-\sin^2(Jt)$	0
$C_{\uparrow\downarrow}$	0	$-\sin^2(Jt)$	$\cos^2(Jt)$	0
$C_{\uparrow\uparrow}$	0	$i \sin(Jt) \cos(Jt)$	$i \sin(Jt) \cos(Jt)$	e^{2iJt}

TABLE I. The time dependent amplitudes $C_{\downarrow\downarrow}, C_{\downarrow\uparrow}, C_{\uparrow\downarrow}, C_{\uparrow\uparrow}$ of the two-qubit state in Eq. (10), for four different inputs $u_{\downarrow\downarrow}, u_{\downarrow\uparrow}, u_{\uparrow\downarrow}, u_{\uparrow\uparrow}$, for a non-interacting, Hermitian system, $g_s = g_c = \gamma = 0$. The table represents the elements of the transformation matrix U .

The precise dynamics of quantum spin system differs from that in Table I, but at time $tJ = \frac{\pi}{2}$ we obtain the equivalent i SWAP gate

$$U_{i\text{SWAP}} = \begin{bmatrix} 1 & 0 & 0 & 0 \\ 0 & 0 & i & 0 \\ 0 & i & 0 & 0 \\ 0 & 0 & 0 & 1 \end{bmatrix}. \quad (13)$$

Consider now the dynamics of the interacting, non-Hermitian \mathcal{PT} symmetric system. For each input state u_i at $t = 0$, the output state $|\Psi_o\rangle$ at time $t > 0$ is

$$|\Psi_o^{(i)}\rangle = C_{\downarrow\downarrow}^{(i)} |\downarrow\downarrow\rangle + C_{\downarrow\uparrow}^{(i)} |\downarrow\uparrow\rangle + C_{\uparrow\downarrow}^{(i)} |\uparrow\downarrow\rangle + C_{\uparrow\uparrow}^{(i)} |\uparrow\uparrow\rangle. \quad (14)$$

We can construct the transformation matrix U as follows: For each input state u_i , the amplitudes of the output state $C_o^{(i)}$ ($i, o \in \{\downarrow\downarrow, \downarrow\uparrow, \uparrow\downarrow, \uparrow\uparrow\}$) constitute the i th column of U . The complete matrix is then obtained by evaluating the dynamics of the system for the four input basis states.

We characterize gate transformation using the fidelity [54],

$$F = \frac{1}{n(n+1)} [\text{Tr}(MM^\dagger) + |\text{Tr}(M)|^2], \quad (15)$$

where $n = 4$ is the size of the Hilbert space (matrix dimension), and $M = U_0^\dagger U$ with U_0 the unitary transformation corresponding to the desired quantum gate, e.g., U_{SWAP} , and U is the actual transformation that we obtain from our simulations. In other words, for any initial state $|\Psi\rangle$, the desired final state is $U_0 |\Psi\rangle$ while the actual state is $U |\Psi\rangle$, and Eq. (15) gives the fidelity of the transformation averaged over all the input states.

The linear \mathcal{PT} case, $g_s = g_c = 0$, is analytically solvable via Eq. (6). At half-period $tJ = \frac{\pi}{2}$ we then obtain the fidelity $F = 0.992$ for $\gamma = 0.1J$. The small reduction of fidelity is due to incomplete population transfer, $\min_t |C_{\downarrow\uparrow(\uparrow\downarrow)}| \simeq \frac{\gamma^2}{J^2 - \gamma^2}$, and a slight shift (stretching) of the oscillation frequency by γ , i.e., the effective Rabi frequency is $\Omega \equiv \sqrt{J^2 - \gamma^2} \simeq J(1 - \gamma^2/2J^2)$. For larger $\gamma = 0.3J$, the fidelity at $tJ = \frac{\pi}{2}$ is further reduced

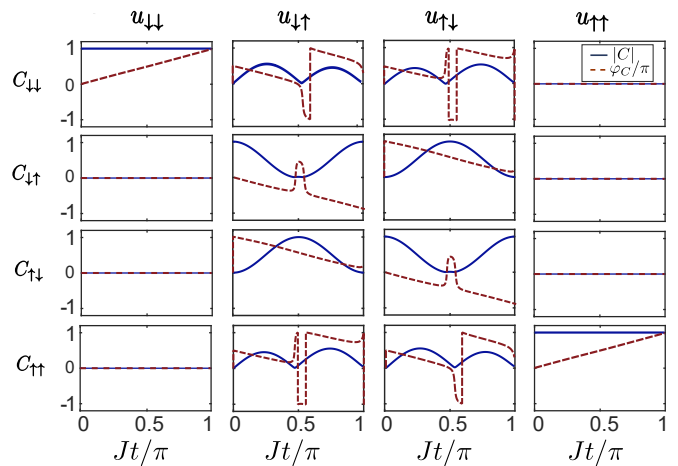


FIG. 4. Time dependence of the complex amplitudes C_o of the output state $|\Psi_o\rangle$ for each input state u_i , up to time $t = \pi/J$, for the system with $g_s N = J$, $g_c N = 0.5J$ and $\gamma = 0.1J$. In each panel, the blue (solid) line is the absolute value of the corresponding amplitude, $|C_o^i|$, and the red (dashed) line is the phase $\phi_C = \arg(C_o^i)$.

to $F = 0.935$. The obtained fidelities can be slightly improved by choosing appropriately delayed SWAP time $tJ = \frac{\pi}{2 - \gamma^2/J^2}$ to compensate for the reduction of the effective Rabi frequency of the oscillations.

We next consider the interacting system with equal self and cross-interaction strengths $g_s N = g_c N = J$ and $\gamma = 0.1J$. This system is not analytically solvable and we numerically calculate the time-dependent amplitudes $C_o^{(i)}$. We obtain fidelity $F = 0.991$ of the SWAP gate at time $tJ = \frac{\pi}{2}$. Further increasing the loss/gain rate decreases the fidelity, e.g., for $\gamma = 0.3J$ we obtain $F = 0.922$, and for $\gamma = 0.5J$ we obtain $F = 0.799$, which can again be improved by using the optimal SWAP times $t = \frac{\pi}{2\Omega}$.

Finally, we examine the general case of unequal self and cross-interaction strengths. Figure 4 shows the evolution of the complex amplitudes $C_o^{(i)}$ for each input state u_i for the system with $g_s N = J$, $g_c N = 0.5J$ and $\gamma = 0.1J$. Each panel of the figure is a direct visualization of the corresponding time-dependent matrix element of transformation U , up to time $tJ = \pi$ of one complete period of population oscillation for the corresponding linear, Hermitian system. At half the period $tJ = \frac{\pi}{2}$, we obtain the SWAP fidelity $F = 0.982$, which is only slightly lower than in the previous cases. With increasing the difference between g_s and g_c the fidelity decreases, albeit rather slowly. For instance, for $g_s N = J$, $g_c N = 0.1J$ the fidelity is $F = 0.963$ for $\gamma = 0.1J$ and $F = 0.867$ for $\gamma = 0.3J$.

VI. CONCLUSIONS

To summarize, we have considered a two-species polariton mixture with self- and cross-interaction nonlinearities in a \mathcal{PT} symmetric double well structure and examined the static and dynamic properties of the system. We have shown that this essentially classical system described by the mean-field coupled-mode equations can nevertheless mimic quantum dynamics of exchange-coupled spins implementing quantum gates.

Our work can be relevant to analog simulations of few-body quantum systems with coupled exciton-polaritons in lattice potentials [15–19]. Thus, one-dimensional polariton lattices can be used to study the dynamics of a single spin excitation, e.g. for the characterization of faithful state or excitation transfer in spin chains with engineered couplings and tunable disorder [55, 56]. Furthermore, the quantum problem of two interacting particles

or spin excitations on a one-dimensional lattice can be mapped onto an appropriately designed two-dimensional lattice of polaritons, similarly to the simulations of the one-dimensional two-particle Hubbard model with two-dimensional arrays of coupled optical waveguides [57–60]. Finally, tunable polariton lattices can serve as versatile simulators of classical spin-lattice models, such as Ising or XY [61–63], which in turn can tackle certain NP-hard optimization problems.

ACKNOWLEDGMENTS

We thank E. Paspalakis for fruitful discussions. This work was co-financed by Greece (General Secretariat for Research and Technology), and the European Union (European Regional Development Fund), in the framework of the bilateral Greek-Russian Science and Technology collaboration on Quantum Technologies (POLISIMULATOR project).

-
- [1] H. Deng, H. Haug, and Y. Yamamoto, *Rev. Mod. Phys.* **82**, 1489 (2010).
 - [2] I. Carusotto and C. Ciuti, *Rev. Mod. Phys.* **85**, 299 (2013).
 - [3] M. Yamaguchi, K. Kamide, R. Nii, T. Ogawa, and Y. Yamamoto, *Phys. Rev. Lett.* **111**, 026404 (2013).
 - [4] C. Schneider, A. Rahimi-Iman, N. Y. Kim, J. Fischer, I. G. Savenko, M. Amthor, M. Lermer, A. Wolf, L. Worschech, V. D. Kulakovskii, I. A. Shelykh, M. Kamp, S. Reitzenstein, A. Forchel, Y. Yamamoto, and S. Höfling, *Nature* **497**, 348 (2013).
 - [5] J. Kasprzak, M. Richard, S. Kundermann, A. Baas, P. Jeambrun, J. Keeling, F. M. Marchetti, M. H. Szymanska, R. André, J. L. Staehli, V. Savona, P. B. Littlewood, B. Deveaud, and L. S. Dang, *Nature* **443**, 409 (2006).
 - [6] R. Balili, V. Hartwell, D. Snoke, L. Pfeiffer, K. West, *Science* **316**, 1007 (2007).
 - [7] G. Lerario, A. Fieramosca, F. Barachati, D. Ballarini, K. S. Daskalakis, L. Dominici, M. De Giorgi, S. A. Maier, G. Gigli, S. Kéna-Cohen, and D. Sanvitto, *Nature Phys.* **13**, 837 (2017).
 - [8] M. Wouters, I. Carusotto, and C. Ciuti, *Phys. Rev. B* **77**, 115340 (2008).
 - [9] C. Trallero-Giner, M. V. Durnev, Y. Nunez Fernandez, M. I. Vasilevskiy, V. Lopez-Richard, and A. Kavokin, *Phys. Rev. B* **89**, 205317 (2014).
 - [10] M. Wouters and I. Carusotto, *Phys. Rev. Lett.* **99**, 140402 (2007).
 - [11] K. G. Lagoudakis, B. Pietka, M. Wouters, R. André, and B. Deveaud-Plédran, *Phys. Rev. Lett.* **105**, 120403 (2010).
 - [12] A. Rahmani and F. P. Laussy, *Sci. Rep.* **6**, 28930 (2016).
 - [13] M. Abbarchi, A. Amo, V. G. Sala, D. D. Solnyshkov, H. Flayac, L. Ferrier, I. Sagnes, E. Galopin, A. Lematre, G. Malpuech, and J. Bloch, *Nature Phys.* **9**, 275 (2013).
 - [14] Rui Zhang, Tao Wang, Zhong Chang Zhuo, Huifang Zhang, and Xue Mei Su, *Opt. Quantum Electron.* **49**, 205 (2017).
 - [15] A. Amo, J. Bloch, *C. R. Physique* **17**, 934 (2016).
 - [16] S. Klemmt, T. H. Harder, O. A. Egorov, K. Winkler, H. Suichomel, J. Beierlein, M. Emmerling, C. Schneider, and S. Höfling, *Appl. Phys. Lett.* **111**, 231102 (2017).
 - [17] C.E. Whittaker, E. Cancellieri, P.M. Walker, D.R. Gulevich, H. Schomerus, D. Vaitiekus, B. Royall, D.M. Whittaker, E. Clarke, I.V. Iorsh, I.A. Shelykh, M.S. Skolnick, and D.N. Krizhanovskii, *Phys. Rev. Lett.* **120**, 097401 (2018).
 - [18] H. Ohadi, Y. del Valle-Inclan Redondo, A.J. Ramsay, Z. Hatzopoulos, T.C.H. Liew, P.R. Eastham, P.G. Savvidis, J.J. Baumberg, *Phys. Rev. B* **97**, 195109 (2018).
 - [19] H. Pan, K. Winkler, M. Powlowski, M. Xie, A. Schade, M. Emmerling, M. Kamp, S. Klemmt, C. Schneider, T. Byrnes, S. Höfling, and N. Y. Kim, *Phys. Rev. B* **99**, 045302 (2019).
 - [20] D. Ballarini, M. De Giorgi, E. Cancellieri, R. Houdré, E. Giacobino, R. Cingolani, A. Bramati, G. Gigli & D. Sanvitto, *Nature Commun.* **4**, 1778 (2013).
 - [21] C. Bender, S. Boettcher, P. Meisinger, *J. Math. Phys.* **40**, 2201 (1999).
 - [22] C.M. Bender, *Rep. Prog. Phys.* **70**, 947 (2007).
 - [23] R. El-Ganainy, K. G. Makris, M. Khajavikhan, Z. H. Musslimani, S. Rotter, and D. N. Christodoulides, *Nature Phys.* **14**, 11 (2018).
 - [24] C.M. Bender, D.C. Brody, and H.F. Jones, *Phys. Rev. Lett.* **89**, 270401 (2002).
 - [25] C.M. Bender, D.C. Brody, and H.F. Jones, *Phys. Rev. D* **70**, 025001 (2004).
 - [26] R. El-Ganainy, K.G. Makris, D.N. Christodoulides and Z.H. Musslimani, *Opt. Lett.* **32**, 2632 (2007).
 - [27] Z.H. Musslimani, K.G. Makris, R. El-Ganainy, and D.N. Christodoulides, *Phys. Rev. Lett.* **100**, 030402 (2008).
 - [28] B. Peng, S. K. Özdemir, F. Lei, F. Monifi, M. Gianfreda, G. L. Long, S. Fan, F. Nori, C. M. Bender and L. Yang, *Nat. Phys.* **10**, 394 (2014).

- [29] X. Zhu, H. Ramezani, C. Shi, J. Zhu, and X. Zhang, *Phys. Rev. X* **4**, 031042 (2014).
- [30] R. Fleury, D. Sounas, and A. Alú, *Nat. Comm.* **6**, 5906 (2015).
- [31] A. Guo, G. J. Salamo, D. Duchesne, R. Morandotti, M. Volatier-Ravat, V. Aimez, G. A. Siviloglou, and D. N. Christodoulides, *Phys. Rev. Lett.* **103**, 093902 (2009).
- [32] C. E. Rüter, K. G. Makris, R. El-Ganainy, D. N. Christodoulides, M. Segev and D. Kip, *Nat. Phys.* **6**, 192 (2010).
- [33] K. G. Makris, R. El-Ganainy, D. N. Christodoulides and Z. H. Musslimani, *Phys. Rev. A* **81**, 063807 (2010).
- [34] K. G. Makris, R. El-Ganainy, D. N. Christodoulides and Z. H. Musslimani, *Phys. Rev. Lett.* **100**, 103904 (2008).
- [35] H. Ramezani, T. Kottos, R. El-Ganainy, and D. N. Christodoulides, *Phys. Rev. A* **82**, 043803 (2010).
- [36] J. D'Ambroise, P. G. Kevrekidis, and S. Lepri, *J. Phys. A* **45**, 444012 (2012).
- [37] F. Yang and Z. L. Mei, *Sci. Rep.* **5**, 14981 (2015).
- [38] T. Kottos, *Nat. Phys.* **6**, 166 (2010).
- [39] K. Li and P. G. Kevrekidis, *Phys. Rev. E* **83**, 066608 (2011).
- [40] K. Li, P. G. Kevrekidis, D. J. Frantzeskakis, C. E. Rüter and D. Kip, *J. Phys. A* **46**, 375304 (2013).
- [41] D. A. Zezyulin and V. V. Konotop, *Phys. Rev. Lett.* **108**, 213906 (2012).
- [42] J.-Y. Lien, Y.eh-N. Chen, N. Ishida, H.-B. Chen, C.-C. Hwang, and F. Nori, *Phys. Rev. B* **91**, 024511 (2015).
- [43] T. Gao, E. Estrecho, K. Y. Bliokh, T. C. H. Liew, M. D. Fraser, S. Brodbeck, M. Kamp, C. Schneider, S. Hfling, Y. Yamamoto, F. Nori, Y. S. Kivshar, A. G. Truscott, R. G. Dall, and E. A. Ostrovskaya, *Nature* **526**, 554558 (2015).
- [44] I. I. Satija, R. Balakrishnan, P. Naudus, J. Heward, M. Edwards, and C. W. Clark, *Phys. Rev. A* **79**, 033616 (2009).
- [45] I. Y. Chestnov, S. S. Demirchyan, A. P. Alodjants, Y. G. Rubo, and A. V. Kavokin, *Sci. Rep.* **6**, 19551 (2016).
- [46] H. Ohadi, A.J. Ramsay, H. Sigurdsson, Y. del Valle-Inclan Redondo, S.I. Tsintzos, Z. Hatzopoulos, T.C.H. Liew, I.A. Shelykh, Y.G. Rubo, P.G. Savvidis, and J.J. Baumberg, *Phys. Rev. Lett.* **119**, 067401 (2017).
- [47] S. Raghavan, A. Smerzi, S. Fantoni, and S. R. Shenoy, *Phys. Rev. A* **593**, 620 (1999).
- [48] E. Estrecho, T. Gao, N. Bobrovska, D. Comber-Todd, M. D. Fraser, M. Steger, K. West, L. N. Pfeiffer, J. Levinsen, M. M. Parish, T. C. H. Liew, M. Matuszewski, D. W. Snoke, A. G. Truscott, and E. A. Ostrovskaya, *Phys. Rev. B* **100**, 035306 (2019).
- [49] B. Deveaud C. R. *Physique* **17**, 874 (2016).
- [50] L. Ferrier, E. Wertz, R. Johne, D. D. Solnyshkov, P. Senellart, I. Sagnes, A. Lematre, G. Malpuech, and J. Bloch, *Phys. Rev. Lett.* **106**, 126401 (2011).
- [51] M. Duanmu, K. Li, R. L. Horne, P. G. Kevrekidis, N. Whitaker, *Phil. Trans. R. Soc. A* **371**, 20120171 (2013).
- [52] M. Albiez, R. Gati, J. Fölling, S. Hunsmann, M. Cristiani, and M. K. Oberthaler, *Phys. Rev. Lett.* **95**, 010402 (2005).
- [53] E-M. Graefe, *J. Phys. A: Math. Theor.* **45**, 444015 (2012).
- [54] L. H. Pedersen, N. M. Møller, and K. Mølmer, *Phys. Lett. A* **367**, 47 (2007).
- [55] D. Petrosyan, G. M. Nikolopoulos and P. Lambropoulos, *Phys. Rev. A* **81**, 042307 (2010)
- [56] G. M. Nikolopoulos and I. Jex (eds.), *Quantum State Transfer and Network Engineering*, Quantum Science and Technology, (Springer, Heidelberg, 2014)
- [57] D. O. Krimer and R. Khomeriki, *Phys. Rev. A* **84**, 041807(R) (2011).
- [58] G. Corrielli, A. Crespi, G. Della Valle, S. Longhi, and R. Osellame, *Nature Commun.* **4**, 1555 (2013).
- [59] A. Rai, C. Lee, C. Noh, and D. G. Angelakis, *Sci. Rep.* **5** 8438 (2015).
- [60] S. Mukherjee, M. Valiente, N. Goldman, A. Spracklen, E. Andersson, P. Ö hberg, and R. R. Thomson, *Phys. Rev. A* **94**, 053853 (2016).
- [61] P. G. Lagoudakis and N. G. Berloff, *New J. Phys.* **19**, 125008 (2017).
- [62] N. G. Berloff, M. Silva, K. Kalinin, A. Askitopoulos, J. D. Töpfer, P. Cilibrizzi, W. Langbein, and P. G. Lagoudakis, *Nature Mater.* **16**, 1120 (2017).
- [63] K. P. Kalinin and N. G. Berloff, *New J. Phys.* **20**, 113023 (2018).